Journal of Sound and Vibration (1999) **226**(5), 941–953
Article No. jsvi.1999.2245, available online at http://www.idealibrary.com on IDEAL®

DYNAMICAL BEHAVIOUR OF THE PLANAR NON-LINEAR MECHANICAL SYSTEM — PART II: EXPERIMENT

M. Boltežar, N. Jakšić, I. Simonovski and A. Kuhelj

University of Ljubljana, Faculty of Mechanical Engineering, Aškerčeva 6, 1000 *Ljubljana, Slovenia*

(*Received* 21 *August* 1998, *and in final form* 16 *March* 1999)

The experimental work has been undertaken on the washing complex dynamics to verify the theoretical approach from Part I. The measured time histories were analyzed by using spectral and phase-space analyses. The correlation dimension and the largest Lyapunov exponent were estimated on a reconstructed phase space through an embedding procedure by using different measured time histories. The largest positive Lyapunov exponent and the non-integer value of the correlation dimension of the attractor confirm the chaotic nature of the washing complex dynamics. The visualization procedure was also implemented in three-dimensional space. Differences were found in the values of the correlation dimension and largest Lyapunov exponent when estimating them from different measured signals. At the same time those estimated values show the same nature of motion. Power spectra and bicoherences have been used to analyze the washing complex dynamical behaviour. It has been found that the dominant mode is the spin-dry frequency, while the higher modes have significantly lower power. The quadratic phase coupling between the second and fifth harmonic is present, thus confirming that the process is non-linear. It is also shown that the bicoherence estimate is sensitive to division by a small number, which can increase its number of peaks. In this case, the magnitude bispectrum has been used to provide a more realistic picture of quadratic phase coupling. The model, described in Part I, is able to simulate the amplitude and the frequency of the predominant harmonic of the washing complex in the steady state, but is unable to simulate all the richness of the motion of the washing complex.

1. INTRODUCTION

In this second part of the paper, experimental results are given to verify the theoretical model as deduced in Part I.

The problem in experimental investigations of frictional systems lies mainly in the very complex frictional mechanism [1–3]. The stick-slip phenomenon was discussed in reference [2] in the case of a single d.o.f. system with one and two stops per half-cycle. Another experimental example was described in reference [4] of the chaotic dynamics of a harmonically forced spring–mass system with dry friction designed to vary linearly with displacement.

0022-460X/99/400941 + 13 $30.00/0

For oscillating systems with several degrees of freedom, the influence of the degree of non-linearity on the integral of correlation dimension (*ICD*) was shown experimentally in the case of a series of coupled rigid bodies [5] in planar motion. On the other hand, the values of the correlation dimension were shown to be dependent on the cutting force in cutting processes where dry friction plays an important role [6]. It was also shown that fault diagnosis of the rolling element bearings may be made by using the correlation dimension [7].

To establish the chaotic nature of the processes, including the friction forces, the Lyapunov exponents were computed [1, 8] from a single measured time history. It was shown that Lyapunov exponents may not be enough to distinguish between the strange chaotic and non-chaotic attractors [1].

Bicoherence measures the phase coherency among three harmonics [9, 10], thus detecting quadratic phase coupling (*QPC*) in a signal. Because machine faults are often associated with some non-linear mode of operation which transfers energy between components of the harmonics, the bicoherence can be used for condition monitoring [11–13]. Bicoherence can be further used to discriminate between phase coupled and randomly excited harmonics and for estimation of the fraction of power due to the *QPC* [10].

In this paper bicoherence has been used to provide additional insight into the washing machine dynamics. Special attention has been given to the statistical stability of the bicoherence estimator and the problem of the division by small number.

2. EXPERIMENTAL SET-UP

The experiment was performed on a washing machine, see Figure 1. As a part of the washing machine, a washing complex is made up of the tub in which the drum is rotating, additional weights and the electromotor attached to the tub and the suspension arms holding the tub as vibroisolation. In the drum of the washing

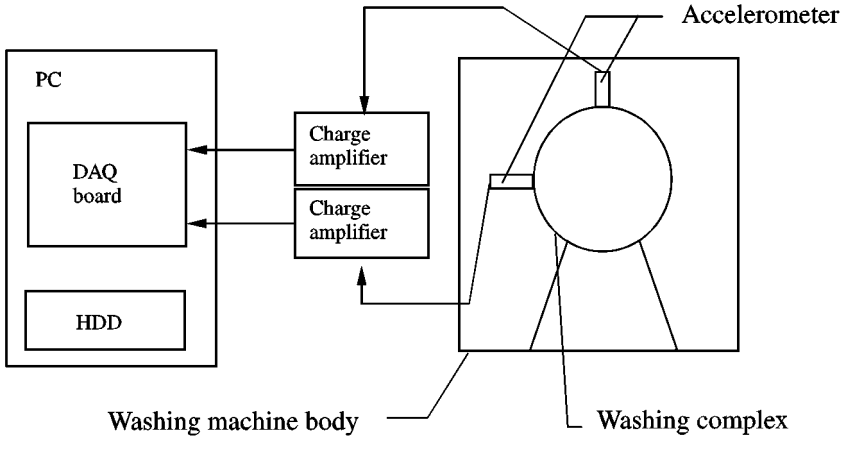

Figure 1. Experimental set-up.

complex at maximum radius an eccentric mass was fixed. In that way the imbalance of the rotating parts was provided and the worst possible laundry distribution was simulated. The system accelerations in vertical and horizontal directions were measured simultaneously using two Brüel and Kjaer (B&K)-type 4367 accelerometers with B&K-type 2635 and 2626 charge amplifiers. The signals were acquired by NI AT-MIO-16E-1 data acquisition board and stored on HDD of a PC for further analysis. The charge amplifier's filter was used for signal conditioning. The low-pass filtering was set at 3 kHz on both charge amplifiers (B&K 2635 and B&K 2626). The sampling frequency was 3 kHz due to aliasing. The signals were resampled to 1 kHz for phase-space analysis.

3. EXPERIMENTAL RESULTS ANALYSIS

The time series of the horizontal (x) and vertical (y) accelerations are presented in Figure 2. The time histories of two simultaneously measured accelerations show that the motion of the washing complex has one dominant frequency; hence, the frequency of spin dry. The signals of accelerations in the horizontal and vertical direction are approximately shifted by $\pi/2$; hence, the washing complex response follows the centrifugal excitation. It was also found that the speed control was able to keep the spin-dry frequency within the range of $\pm 1\%$, compared to the set spin-dry frequency.

3.1. SPECTRAL ANALYSIS

Power spectra were calculated by using 4096 FFT points. Overlapping of 5% was used to obtain 128 segments, and the Hamming window was applied in the time domain. A fourth order lowpass elliptic digital filter was used with a cut-off frequency of 300 Hz with approximately linear-phase characteristics. The power spectra of horizontal and vertical acceleration are presented in Figures 3 and 4. In both the horizontal and vertical direction the spin-dry frequency of 17·58 Hz is clearly visible. The third harmonic, generated by the three-arm support of the drum, has already 70 dB lower power. In Figure 4, peaks at 145·02 and 208·01 Hz can be observed. The cause of these two peaks is unknown. At other frequencies the spectral power is significantly lower.

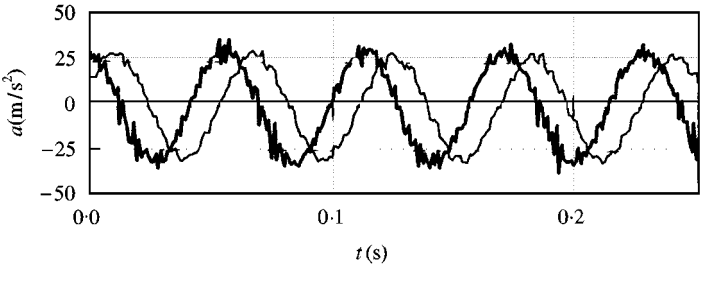

Figure 2. Measured steady state accelerations. —, a_x; —, a_y.

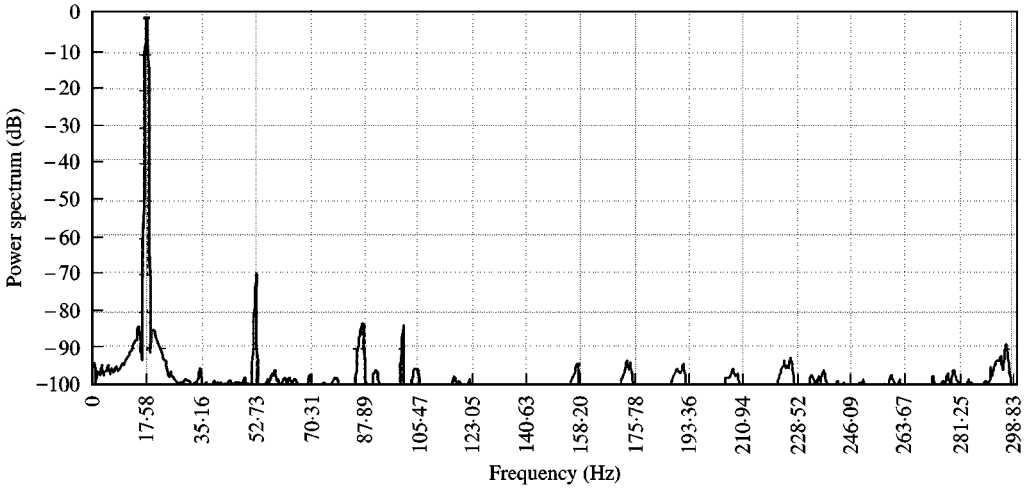

Figure 3. Power spectrum of the measured horizontal accelerations.

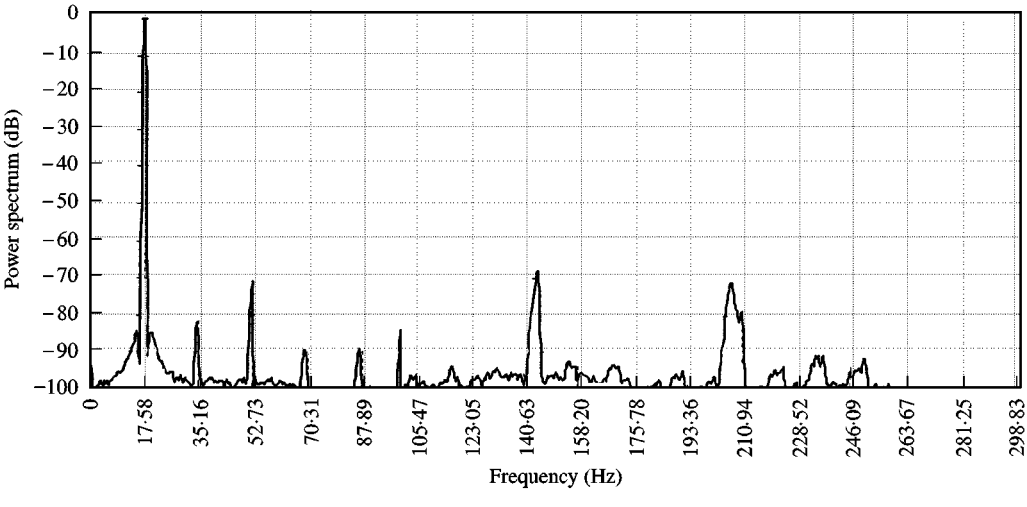

Figure 4. Power spectrum of the measured vertical accelerations.

The bicoherences of horizontal and vertical measured accelerations were calculated using the same parameters as described in Part I, and are presented in Figures 5 and 7. The number of FFT points per segment was 1024; the 5% overlapping was used to obtain 513 segments. Because of its ability to resolve *QPC* peaks [14, 15], the Hamming window was applied in the time domain. The bicoherence significance of $T_{\alpha\%} = 95\%$ was used to determine the minimal significant bicoherence level. Biphase significance was not used because it was found that the probability distribution of the biphase did not comply with the normal distribution. The numerical zero threshold was set to 1E-10.

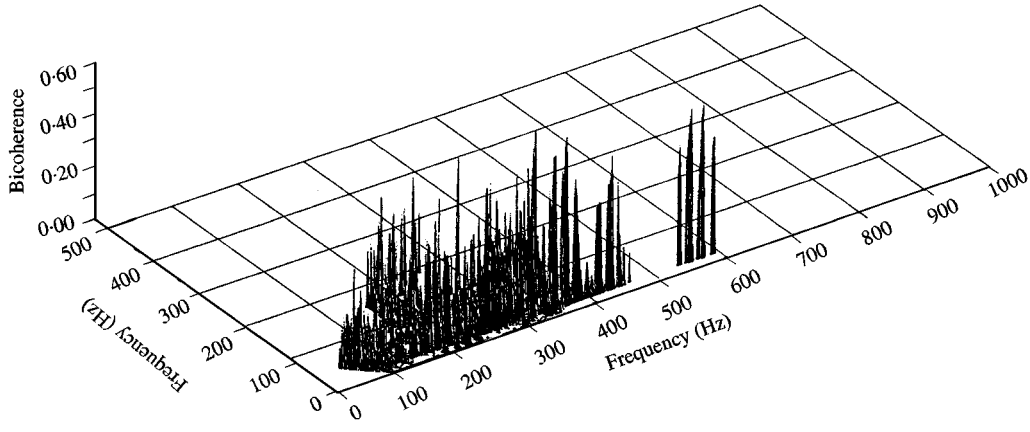

Figure 5. Bicoherence surface plot of the measured horizontal acceleration.

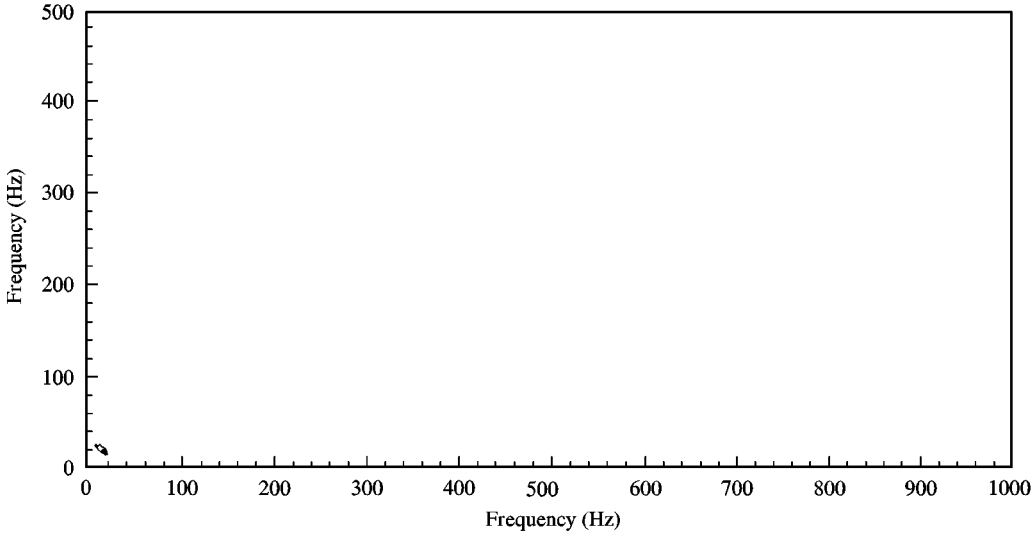

Figure 6. Magnitude bispectrum contour plot of the measured horizontal accelerations. The maximum value is 1·45, minimum and maximum contour values are 0·2 and 1·4.

One can see that the bicoherence of the horizontal acceleration has multiple peaks, scattered over the most part of the IT. The numerous peaks are probably caused by the division with small number, especially because the magnitude bispectrum exhibits only one peak of 1·45 at (17·58, 17·58) Hz; see Figure 6. Although the variance of the bispectrum is dependent upon the signal's second order properties, the large number of segments should minimize this influence. The bicoherence of the vertical accelerations gives a much clearer picture of *QPC*. Four distinct bicoherence values stand out; see Table 1. The second harmonic has very little power and can be observed only on the power spectrum of the vertical accelerations in Figure 4. The little power it has, is 63% due to the *QPC* of the

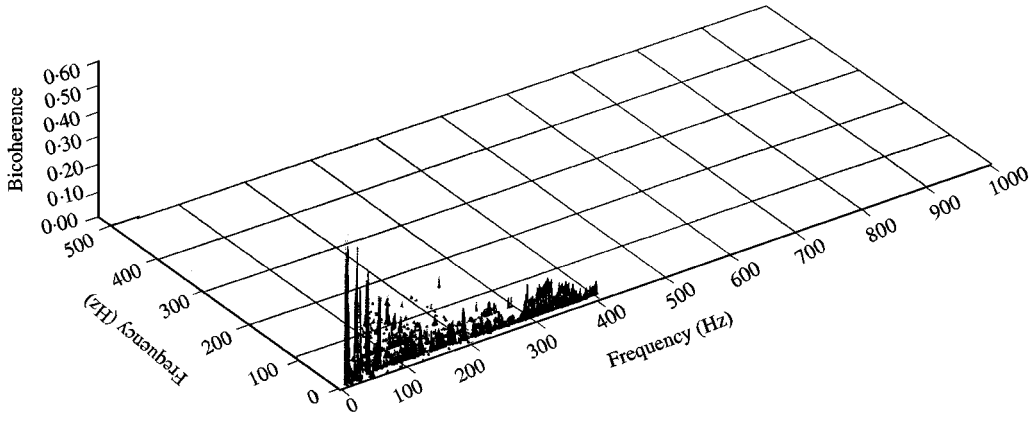

Figure 7. Bicoherence surface plot of vertical acceleration.

TABLE 1

The highest bicoherence values of vertical accelerations

Bicoherence	Frequency (Hz)	Frequency sum (Hz)	Harmonic
0·63	(17·58, 17·58)	35·16	2
0·51	(35·16, 17·58)	52·73	3
0·41	(52·73, 17·58)	70·31	4
0·31	(52·73, 35·16)	87·89	5

spin-dry frequency. The third harmonic (≈ -70 dB) is 49% generated by the three-arm support of the drum and 51% generated by *QPC* of the spin-dry frequency and second harmonic. Similarly, 41% of the fourth and 31% of the fifth harmonic's power is due to the *QPC*. These values confirm that the process involved is not linear and that quadratic non-linearities are present. In Figure 5, a peak in the higher frequency domain (up from 300 Hz) can be seen. This is due to the magnitude characteristic of the digital filter used and division by small number when normalizing. The filter's magnitude response starts to fall at 300 Hz, and only reaches values close to zero at 500 Hz. In this case both the numerator and denominator of the bicoherence are larger than the zero threshold, so that the algorithm cannot filter out these values. This translates into the peak seen in Figure 5.

3.2. PHASE-SPACE ANALYSIS

In experimental work the real phase space is almost always unknown, and the phase space could be reconstructed through the embedding procedure described in Part I.

3.2.1. *Correlation dimension*

To characterize the dimensionality of an attractor in reconstructed phase space the integral of correlation dimension was used. The formulae are presented in Part I.

The estimates of the correlation dimension were computed by employing a reconstruction procedure on the experimental time histories of the horizontal and vertical washing complex accelerations. The correlation dimensions were extracted as $v = 1{\cdot}51 \pm 0{\cdot}02$ and $1{\cdot}24 \pm 0{\cdot}01$ respectively. The differences in the correlation dimension estimates are due to the fact that each signal carries the signature of the entire dynamics of the system, although the dynamics of the measured direction has a greater importance. It was shown [3] that the dynamics in the horizontal direction is richer than that in the vertical direction. In both cases estimates of the correlation dimension show that the attractor is topologically a fractal object.

The first log–log diagram of the integral of the correlation dimension based on the horizontal acceleration is shown in Figure 8, and the second one based on the vertical acceleration is shown in Figure 9. The interesting part of the diagrams lies above the point where the lines of the integral of correlation dimension computed with different embedding dimensions converge. The lower part of the diagrams, with regard to the characteristic distance L, shows the typical dependence of the correlation dimension on white noise hidden in the measured signal [16]. All of the plots in Figures 8 and 9 are based on a computation using 5000 points [17] when reconstructing the phase space.

3.2.2. *Lyapunov exponents*

The Lyapunov exponents measure the exponential divergence (positive exponents—chaotic motion) or convergence (negative exponents—regular motion) of two initially neighbouring trajectories in the phase space.

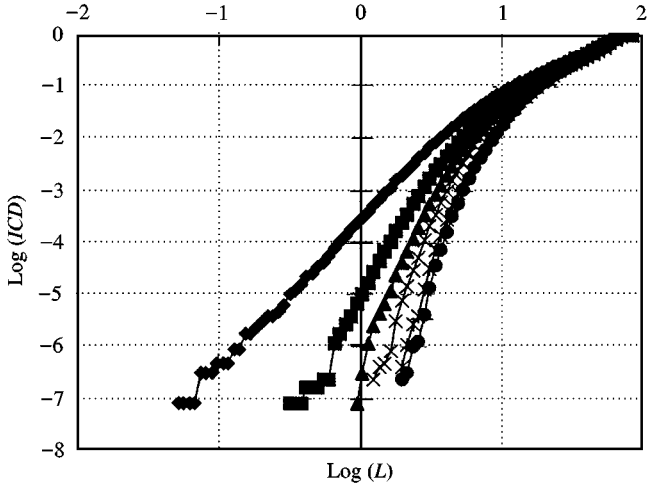

Figure 8. *ICD* on measured horizontal accelerations of the washing complex. —— *d* values; –◆–, 3; –■–, 5; –▲–, 7; –×–, 9; –∗–, 13; –●–, 15.

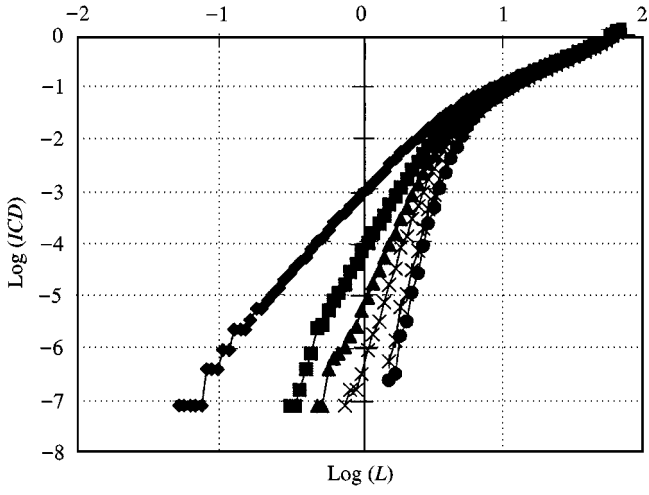

Figure 9. *ICD* on measured vertical accelerations of the washing complex. —— *d* values; -◆-, 3; -■-, 5; -▲-, 7; —×—, 9; —∗—, 13; -●-, 15.

The technique [18] for computing the largest positive Lyapunov exponent from small data sets has been used. The method locates the nearest neighbour to the reference point using the Euclidean norm and so defining the initial distance between the points. The method imposes additional constraints; hence, the nearest neighbour should have a temporal separation greater than the mean period of the time series. Consequently, the two neighbouring points could be treated as nearby initial conditions for two different trajectories. The largest Lyapunov exponent is then estimated as the mean rate of separation of the neighbours. The algorithm is unable to compute negative Lyapunov exponents.

The estimates of the largest Lyapunov exponent were computed by employing a reconstruction procedure on the experimental time histories of the horizontal and vertical washing complex's accelerations. The largest Lyapunov exponents were estimated as $\lambda_{\max,x} = 0{\cdot}20 \pm 0{\cdot}00$ and $\lambda_{\max,y} = 0{\cdot}16 \pm 0{\cdot}00$, respectively, as the inclination of the slope of the linear regression line imposed on plots in Figures 10 and 11, respectively, for $d = 9$. The differences in Lyapunov exponent estimates are due to the same phenomena as described in case of the correlation dimension estimation. It is shown again that the processes in the horizontal direction are more "turbulent" than those in the vertical direction.

To check for spurious Lyapunov exponents the time flow of processes was reversed [19]. It would be normal, if the computed Lyapunov exponents were not spurious, to expect negative estimates of the largest Lyapunov exponents of both processes when time is reversed. Since the method is unable to compute negative Lyapunov exponents, the almost zero value of both the largest Lyapunov exponents of reverse processes was estimated; see Figures 12 and 13. Hence the estimation of the largest Lyapunov exponents of the accelerations' time histories shows that they are not spurious and the dynamics of the washing complex appears to be chaotic.

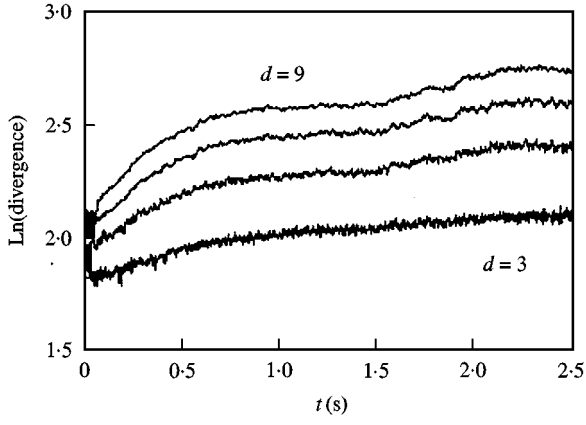

Figure 10. Divergence of trajectories on measured horizontal accelerations of the washing complex.

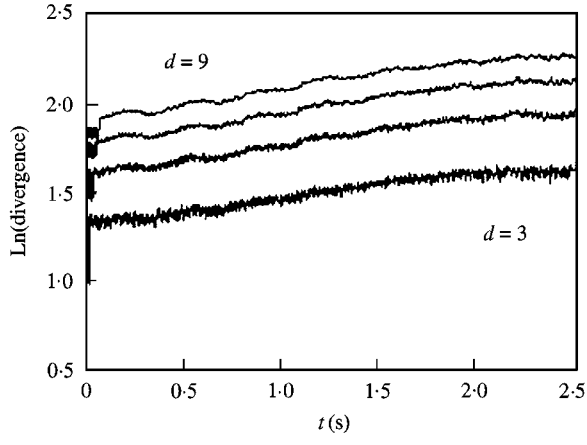

Figure 11. Divergence of trajectories on measured vertical accelerations of the washing complex.

All of the plots in Figures 10–13 are based on a computation using 5000 points of reconstructed phase space [17].

3.2.3. *Attractor visualization*

In the case of experimental data the visualization could be done through the embedding procedure as described in Part I.

The visualized attractor from the horizontal acceleration's time history in three-dimensional space, $d = 3$, is shown in Figure 14, and the visualized attractor from the vertical acceleration's time history in three-dimensional space, $d = 3$, is shown in Figure 15.

The washing complex attractor is torus-shaped; this is due to the one predominant harmonic which is driven by spin dry. It is also visible that the

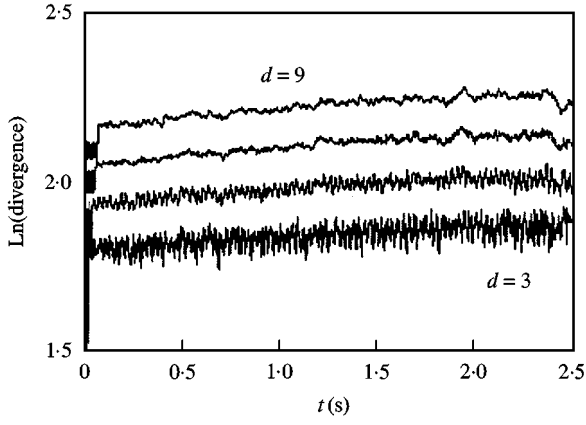

Figure 12. Divergence of trajectories on reversed signal of horizontal acceleration of the washing complex.

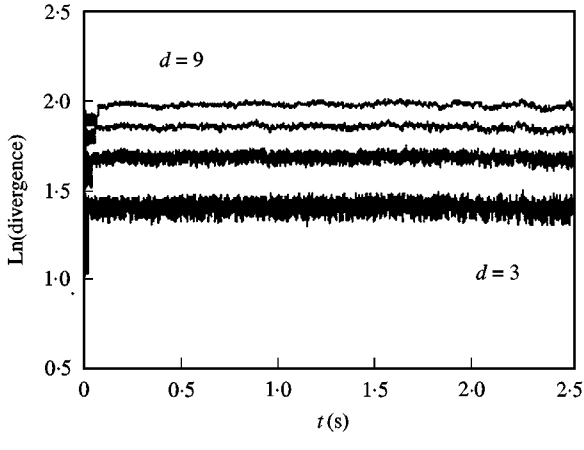

Figure 13. Divergence of trajectories on reversed signal of vertical acceleration of the washing complex.

dynamics in the horizontal direction are more widely dispersed around the predominant harmonic's limit cycle than in the vertical direction. This is in agreement with results of analysis of the attractor's dimensionality and of the Lyapunov exponents.

4. CONCLUSIONS

The steady state responses of the washing-machine washing complex oscillations were analyzed. The results of the simulations and experiment have been compared.

The estimates of the correlation dimension are revealed on the fractal structured attractor of the washing complex dynamics. This is consistent with the estimates of

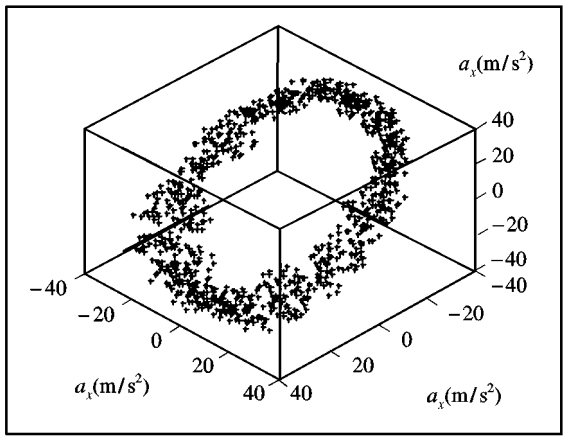

Figure 14. Visualization of the washing complex attractor from the horizontal acceleration's time history.

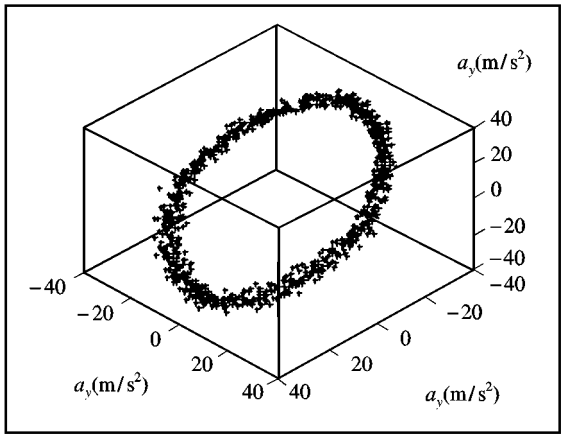

Figure 15. Visualization of the washing complex attractor from the vertical acceleration's time history.

the largest Lyapunov exponent. Its positive value reveals the chaotic nature of the attractor. The visualization of the attractor shows its torus-shape, which is due to one predominant harmonic driven by spin dry, and the dispersion around the predominant harmonic's limit cycle, which is due to the chaotic nature of motion.

In all cases of phase-space analysis the difference between dynamics in the vertical and horizontal direction is clearly visible. The difference is due to the fact that each signal carries the signature of the entire dynamics of the system, although the dynamics of the measured direction has a greater importance. Nevertheless, each of the signals carries enough of the system's dynamics to enable all phase-space analyses, regardless of the direction of the processed time history, to show the same nature of the washing complex motion.

In spite of the chaotic nature of washing complex motion, the power spectra do not appear to be continuous due to the predominant harmonic. The power spectra of such processes could be easily mistaken for a quasi-periodic one.

Bispectral analysis has also been performed on the measured horizontal and vertical accelerations of the washing complex oscillations. Due to the poor statistical properties of the bispectral estimate, bicoherence has been used as a means of detecting *QPC*. It has been found that the division by small numbers can have a great influence on this estimate. The division by small numbers increases the number of *QPC*, detected by bicoherence estimate, and is demonstrated in the large number of bicoherence peaks. To overcome this problem, a numerical threshold for zero value has been introduced. Whenever the numerator of the bicoherence is smaller than this threshold, bicoherence is set to zero. If on the other hand the numerator is greater and the denominator is smaller than the threshold, a small constant value is added to the denominator. It has also been found useful to check the magnitude bispectrum. All the bicoherences presented are to the some degree influenced by the division by small numbers. When comparing the results of the model and experiment, the latter suggest that the theoretical model is not complex enough and exhibits less *QPC*. The experimental results show that the third, fourth and fifth harmonic are not independent, but are to the small extent the result of the *QPC*.

The discrepancy between the model and experiment could be attributed to our not being able to model in every single detail such a complex device as the washing machine. For example, the real electromotor is capable of holding a constant spin-dry speed in the range of $\pm 1\%$ of the declared speed. The supports contain some elastomeric parts that were modelled only by their frictional properties. In our case, we found that even the nature of motion of the model and the washing complex is not the same, but that the model well reflects the steady state motion of the washing complex in the frequency and time domains.

REFERENCES

1. R. Barron, J. Wojewoda J. Brindley and T. Kapitaniak 1993 *Journal of Sound and Vibration* **162**, 369–375. Interpretation of aperiodic time series: a new view of dry friction.
2. J. P. Den Hartog 1931 *Transactions of The ASME* **53**, 107–115. Forced vibrations with combined coulomb and viscous friction.
3. N. Jakšić 1997 *M.Sc. Thesis, University of Ljubljana, Faculty of Mathematical Engineering*. Vibration analysis of the nonlinear centrifugally excited planar system (in Slovene).
4. B. Feeny and F. C. Moon 1994 *Journal of Sound and Vibration* **170**, 303–323. Chaos in a forced dry-friction oscillator: experiments and numerical modelling.
5. M. Boltezar and J. K. Hammond 1994 *Fifth International Conference on Recent Advances in Structural Dynamics, ISVR, Southampton*, 18–21 *July, Proceedings* 305–315. Experimental analysis of a multi-degree-of-freedom nonlinear mechanical system.
6. I. Grabec 1988 *International Journal of Machine Tools and Manufacturing* **28**, 19–32. Chaotic dynamics of the cutting process.
7. D. Logan and J. Mathew 1996 *Mechanical Systems and Signal Processing* **10**, 251–264. Using the correlation dimension for vibration fault diagnosis of rolling element bearings — II. Selection of experimental parameters.

8. M. Boltezar and N. Jakšić 1998 *Zeitschrift für Angewandte Mathematik und Mechanik*, **78**, 287–288. Quantitative phase space analysis of the nonlinear planar oscillatory system.
9. C. H. Nikias and A. P. Petropulu 1993 *Higher-Order Spectra Analysis, A Nonlinear Processing Framework*. Englewood Cliffs, NJ: *Prentice-Hall*.
10. Y. C. Kim and E. J. Powers 1979 *IEEE Transactions on Plasma Science* **PS-7**, 120–131. Digital bispectral analysis and its application to nonlinear wave interactions.
11. J. W. Fackrell, P. R. White, J. K. Hammond, R. J. Pinnington and A. T. Parsons 1995 *Mechanical Systems and Signal Processing* **9**, 267–274. The Interpretation of the bispectra of vibration signals—II. Experimental results and application.
12. R. W. Barker and M. J. Hinich 1993 Tahoe, *IEEE Signal Processing Workshop on Higher-Order Statistic* 187–191. Statistical monitoring of rotating machinery by cumulant spectral analysis.
13. T. W. S. Chow and G. Fei 1995 *IEEE Transactions on Energy Conversion* **10**, 688–693. Three phase induction machines asymmetrical faults identification using Bispectrum.
14. J. W. Fackrell 1996 *Ph.D. thesis, The University of Edinburg*. Bispectral analysis of speech signals.
15. I. Simonovski 1998 *M.Sc. Thesis, University of Ljubljana, Faculty of Mechanical Engineering*. Third order spectra analysis of nonlinear dynamical systems (in Slovene).
16. J. P. Eckmann and D. Ruelle 1985 *Reviews of Modern Physics* **57**, 617–655. Ergodic theory of chaos and strange attractors.
17. J. P. Eckmann and D. Ruelle 1992 *Physica D* **56**, 185–187. Fundamental limitations for estimating dimensions and Lyapunov exponents in dynamical systems.
18. M. T. Rosenstein, J. J. Collins and C. J. De Luca 1993 *Physica D* **65**, 117–134. A practical method for calculating largest Lyapunov exponents from small data sets.
19. U. Parlitz 1991 *International Journal of Bifurcation Chaos* **2**, 155–165. Identification of true and spurious Lyapunov exponents from time series.